J. Fluid Mech. (2023), *vol*. 962, A37, doi:10.1017/jfm.2023.172

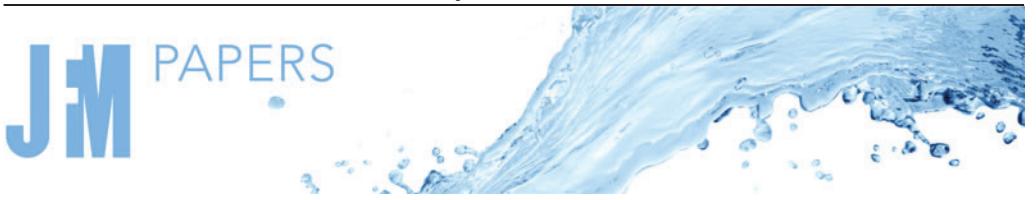

Optimal control of tidal flow

Christian Schmitz[1] **and Peter F. Pelz**[1],†

[1]Chair of Fluid Systems, Technische Universität Darmstadt, Otto-Berndt-Straße 2, 64287 Darmstadt, Germany

(Received 11 February 2022; revised 15 February 2023; accepted 15 February 2023)

The tidal flow through a channel connecting two basins with different tidal regimes can be optimally controlled by means of a turbine fence or array to maximise the extracted mechanical power. The paper gives the optimal control strategy as a function of the blockage ratio σ, i.e. the ratio of the turbine cross-section to the cross-section of the local passage of a turbine. The results presented are a physically consistent generalisation of the results of Garrett & Cummins (*Proc. R. Soc. Lond.* A, vol. 461, 2060, pp, 2563–2572), valid only for $\sigma = 1$ and turbine efficiency of one, now for arbitrary blockage ratio $0 < \sigma \leqslant 1$. Published research over the past decade on the same topic has taken the momentum equation and the turbine drag force as a starting point. The new approach presented here, in contrast, takes the energy equation as the starting point and uses the relative volume flow as the control variable. As the work shows, this new approach has three advantages. First, starting with the energy equation allows us to derive an optimal flow control problem resulting in an Euler–Lagrange equation using the physically consistent and experimentally validated actuator disk model for the free surface flow of Pelz *et al.* (*J. Fluid Mech.*, vol. 889, 2020) in a direct and formal way. The optimal control problem is solved (*a*) numerically and (*b*) analytically. In the latter case, the turbine characteristics are approximated by a rational function in the relevant design and operating range. The analytical solution (*b*) validated against the numerical solution (*a*) is surprisingly concise and easy to apply in practice, as shown by use cases. Second, instead of the induction factor, we use the volume flow that is the same for all turbines in a cascade, i.e. a row of turbines in the direction of flow, which significantly reduces the complexity of the optimal control task of turbine arrays. Third, we obtain a well-founded energy estimate, whereas previous methods overestimate the energy yield due to inconsistent turbine disc models (for the consistency and valid parameter ranges of different models, also in comparison with experiments, see Pelz *et al.*, *J. Fluid Mech.*, vol. 889, 2020). The results can be used for the conceptual design of turbine arrays, but also for a sound physically realistic and consistent resource assessment of tidal power for a system consisting of two basins, a channel and a turbine fence with $0 < \sigma \leqslant 1$ and operated in a complete tidal cycle.

† Email address for correspondence: peter.pelz@tu-darmstadt.de

Key words: channel flow, hydraulics

1. Introduction

Low head hydropower such as tidal power offers a contribution to meet the world's rising electrical power demand, as long as the technology becomes economically viable (Rourke, Boyle & Reynolds 2010). For power extraction, axial turbines have been or may be installed at several promising sites on Earth. Many of these are narrow channels or straits between two basins with different tidal regimes, cf. figure 1. For the evaluation of tidal channels that are considered as sites for turbine fences or turbine arrays, the usable energy to be harvested from the tidal stream is of central interest.

First assessments used the so-called 'farm method', which were solely based on the energy flow through the channel undisturbed by any turbine. By ignoring the physically relevant slowing of the tidal stream by the turbines, the method is only a summation of nominal powers, leading to a vast overestimation of the tidal resource (Black & Veatch Consulting Ltd 2005).

Garrett & Cummins (2005) recognised the limitations of this method and in contrast considered a flow reduction due to the turbine's operation from the undisturbed volume flow Q_0, i.e. the volume flow within the tidal channel without any turbine, to the volume flow within the channel Q. The volume flow reduction is measured via the relative volume flow rate

$$0 < q(t) := \frac{Q(t)}{Q_0(t)} \leqslant 1, \tag{1.1}$$

and is controlled by the realised turbine array. They derived an upper limit, i.e. a factor 0.21 to 0.24 of the maximum energy flow $\hat{P}_{D,0} = \varrho g \hat{Q}_0 \Delta\hat{H}$, by analysing the response of the tidal system, i.e. the control volume (CV) labelled by CV I-II in figure 1, to a zero-loss turbine fence. Here, ϱ is the water density, g is the magnitude of the mass-specific gravity vector, $\hat{Q}_0$ is the peak volume flow in the tidal cycle without a turbine installed and $\Delta\hat{H}$ is the peak difference in energy head between the two ends of the tidal channel.

For such an idealised fence, there are neither internal losses within the turbines, i.e. a turbine efficiency $\eta_T = 1$, nor external losses $P_{D,M}$ due to mixing of bypass and turbine volume flow downstream of the turbine fence. This is only valid for full blockage of $\sigma = 1$, with the blockage ratio σ defined as usual (Garrett & Cummins 2007; Houlsby, Draper & Oldfield 2008; Whelan, Graham & Peiró 2009; Pelz *et al.* 2020) as the ratio of the turbine's projected area A_T to the passage cross-sectional area A_1, cf. figure 1,

$$0 < \sigma := \frac{A_T}{A_1} \leqslant 1. \tag{1.2}$$

The 'flux method' of Garrett & Cummins (2005) was first applied by Black & Veatch Consulting Ltd (2005), using an iterative combination of flux and farm method to take the additional practical limitation of incomplete blockage into account. With a constrained relative volume flow by a lower bound of $0.9 \leqslant q$ – for ecological reasons – the maximum power output out of tidal stream sites was estimated to amount to $C_W = 8.6\,\%$. This is therefore the extractable fraction of the reference power $\hat{P}_{D,0}$. As a result, the projected usable tidal energy per year on the coasts of the United Kingdom has been reduced from formerly 58 TWh a^{-1} (ETSU 1993) to only 18 TWh a^{-1} (Black & Veatch Consulting Ltd 2005).

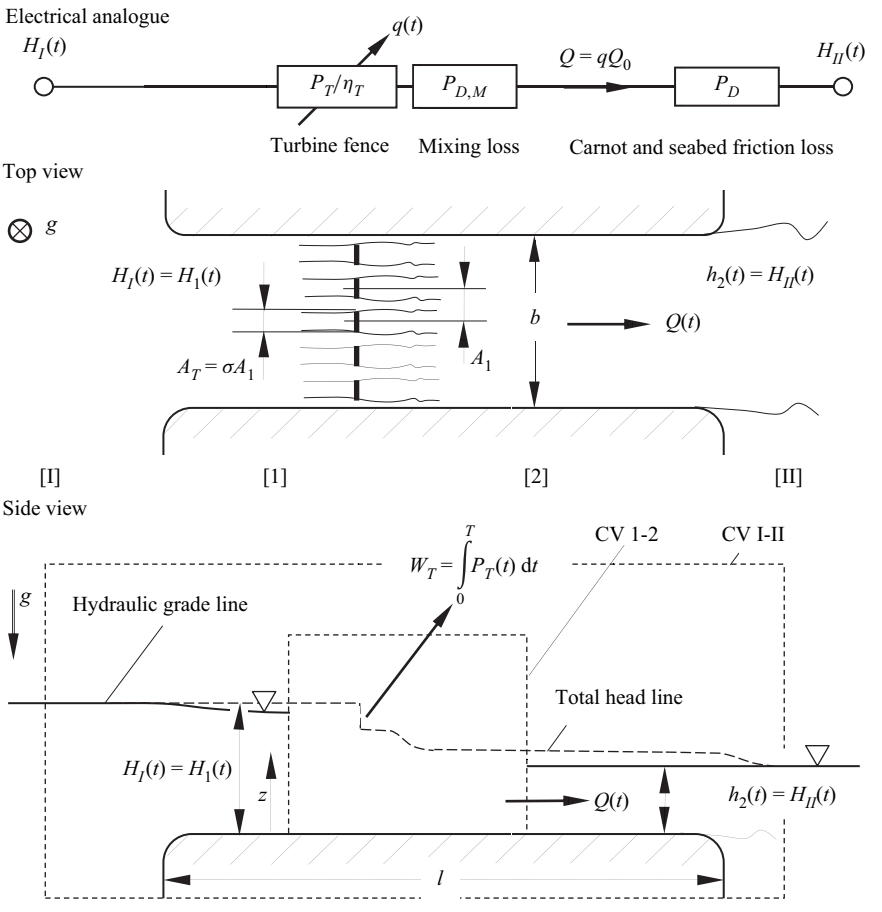

Figure 1. Top and side views of a generic tidal channel as well as the electrical analogue. The energy is extracted by a regular turbine fence with partial blockage ratio $0 < \sigma := A_T/A_1 \leqslant 1$ with subsystem CV 1-2 and system CV I-II being in focus of this paper.

The fraction C_W was originally introduced as the significant impact factor by Black & Veatch Consulting Ltd (2005). However, since it is an energy coefficient, we use the more appropriate term C_W. One might argue in favour of calling the mentioned fraction efficiency. In energy systems, however, the term efficiency is usually used to measure the dissipation within a system boundary, e.g. within CV 1-2 depicted in figure 1. In the context of this paper, the minimisation of the flow of unused exergy across the system boundary is decisive for the energetic optimality of the system. Following Betz (1920) and as is usual for energy systems, we therefore distinguish between the efficiency η (e.g. (1.9) and (2.21)) and the coefficient of performance, which is either an energy coefficient C_W introduced for the system labelled by CV I-II (e.g. (1.6) and (1.7)) or a power coefficient C_P introduced for CV 1-2.

1.1. *Overview of existing turbine disc models (CV 1-2)*

The effect of blockage on the power coefficient C_P for CV 1-2, namely the interaction of the turbine with the lateral channel boundaries, was first studied by

Garrett & Cummins (2007). They considered a Rankine–Froude momentum actuator disc in a simplified channel with fixed water depth $h_1 = h_2$ and thus no influence of gravity on the free surface. Essentially, even this simplest turbine disk model captures dissipation due to mixing of flow through the turbines and flow bypassing the turbines. This mixing causes considerable energy losses that are lost for power generation. To minimise these losses, the turbines must be optimally tuned. According to Garrett & Cummins (2007), the power output is maximised by tuning the axial induction factor, defined by $\alpha := u_w/u_1$, to the same optimal value as that found by Lanchester (1915) and Betz (1920) to be valid for turbines in unbounded flow, i.e. $\alpha_{opt} = 1/3$ for the special case $\sigma \to 0$. Here, u_1 is the velocity of the incoming flow far upstream of the turbine fence and u_w is the flow velocity in the turbine's wake.

Past work has shown that the assumption $h_1 = h_2$ is in contradiction with the conservation of energy, which tends to lead to an overestimation of the energy yield (Pelz *et al.* 2020). Hence, there is a need for improved coarse-grained and fine-grained turbine disk models. On the one hand, sound coarse-grained turbine disk models are needed for three reasons: first, for the initial estimation of the potential energy yield of a tidal channel, second, for the conceptual design phase of the turbine array required for this and, third, for the model predictive control of the turbines in the usage phase. On the other hand, for the subsequent embodiment design phase (Pahl *et al.* 2007) of the turbines, fine-grained turbine models based on boundary or volume element methods are required (Vogel, Willden & Houlsby 2019; Ouro & Nishino 2021).

For the conceptual design and resource estimation the model of Garrett & Cummins (2007) was refined by Whelan *et al.* (2007, 2009), Houlsby *et al.* (2008) and Pelz *et al.* (2020), taking into account the deformation of the free surface by gravity, i.e. $h_1 \neq h_2$.

An in-depth analysis shows that the turbine disc models of Garrett & Cummins (2007), Whelan *et al.* (2007, 2009) and Houlsby *et al.* (2008) conflict with either the continuity equation (Garrett & Cummins 2007) or the energy equation (Houlsby *et al.* 2008; Whelan *et al.* 2009). All named turbine disk models overestimate the energy yield compared with a generic real experiment. Only the turbine disk model by Pelz *et al.* (2020) shows convincing results in the entire range of upstream and downstream boundary conditions. This model was developed specially for flows with free surfaces, whereby particular attention was paid to conservation laws. Both models, the special model for $\sigma = 1$ (Pelz 2011) and the generalised model for $0 < \sigma \leqslant 1$ (Pelz *et al.* 2020), consider the contraction of the turbine streamtube due to the water head drop above the turbine and the associated change in flow of kinetic energy and momentum across the turbine. Both turbine disc models are for a steady or quasi-steady flow between cross-sections 1 and 2, cf. figure 1.

Schmitz & Pelz (2021) generalised the results of Pelz *et al.* (2020) valid for one turbine fence to a cascade of $L = 1, 2, 3, \ldots$ turbine fences forming a regular turbine array within the subsystem CV 1-2. The authors report that even for identically designed fences, each fence has to be operated differently to achieve optimal tuning due to the changing water depth over the turbine array. This corrects the statement that all turbines are operated in the same way by Vennell (2010*a*), whose conclusion is consistent only with the very simple turbine model of Garrett & Cummins (2007) but does not apply to the more physical model of Pelz *et al.* (2020). Schmitz & Pelz (2021) further state that the relative gain of added rows becomes smaller the more rows are added. As a consequence, even for a hypothetical array with an infinite number of rows, the maximum power output is limited by the power gained with a single fence of full blockage $\sigma = 1$ derived by Pelz (2011).

1.2. *Overview of existing channel models (CV I-II)*

A combination of a model for CV 1-2 and the flux method introduced by Garrett & Cummins (2005) for CV I-II was first done by Vennell (2010*a*) using the induction-factor-dependent drag force from the simple turbine disc model of Garrett & Cummins (2007). Vennell (2010*a*) rightly points out, that the tidal channel's energy potential depends on properties of the channel only and not on the array's design and operation, whereas the harvestable fraction does. The results show, as intuition would indicate, that the exploitable fraction of the channel's energy potential C_W is higher if more turbines are installed, especially, if the array is designed in a way to occupy most of the channel's cross-section, i.e. following the paradigm 'filling rows first, then adding rows up'. Vennell (2010*a*) further notices, that the optimal tuning of the turbines depends on the topology of the array on the one hand and the channel's properties on the other hand. He derives the optimal axial induction factor to be approximately $\alpha_{opt} \approx 1/3$ being the same for all turbine of a 'small' turbine array and $\alpha_{opt} \approx 1$ for all turbines of a 'large' turbine array.

Vennell (2010*b*) extends the analysis to non-uniform channels with a constriction in width.

Vennell & Adcock (2013) and Vennell (2016) point out that the power output can be enhanced when using the inductance of the channel flow by smart operation of the tidal turbines. This interesting approach is very shortly discussed in § 2.2.

Nishino & Willden (2012, 2013) and Vogel, Houlsby & Willden (2016) bring attention to the fact that the energy extraction can be enhanced by asymmetric turbine arrays, as an additional bypass around the turbine array can be beneficial for energy extraction. This effect can be pushed to its limits, as Dehtyriov *et al.* (2021) have recently shown. The influence of centred and staggered arrangements is discussed e.g. by Draper *et al.* (2014).

There are many further works on the solution of field equations, i.e. the shallow water equations in two space dimensions (Vogel *et al.* 2019; Bonar *et al.* 2019); or the Navier–Stokes equations in three space dimensions with detailed modelling of the machine–fluid interaction, e.g. Ouro & Nishino (2021). These kinds of analyses are important for the detailed optimisation of turbines or the application of turbines to specific channels.

As mentioned earlier, the motivation of this paper is to improve the basis for conceptual design. Therefore, blade element theory, boundary element methods or volume methods are mentioned as important methods here. However, they will not be considered further in the remainder of this paper.

1.3. *Approach, objective, open research question, presentation and structure of the paper*

To be concise, without contradiction to energy and mass conservation, the new approach presented here takes the energy equation for the system CV I-II – not the momentum equation as in previous works in the sequence of Betz (1920) being valid only for $\sigma \to 0$ – as the starting point. As mentioned, this new approach for arbitrary blockage ratio, $0 < \sigma \leqslant 1$, for the system labelled CV I-II has three advantages. First, starting with the energy equation allows us in a strict, direct and formal way to end up with an optimal control problem. This leads us to the three necessary conditions indicating a quasi-steady channel flow. The optimal control problem is solved (*a*) numerically and (*b*) analytically for this quasi-steady flow. Second, instead of the axial induction factor, we use the volume flow that is the same for all turbines in a cascade, reducing the number of controlled variables of a turbine array. In addition, using the volume flow as a control

parameter simplifies the problem considerably, as the boundary conditions only enter the problem via the relative volume flow. Third and finally, we obtain a well-founded energy estimate.

The paper is in line with those of Vennell (2010*a*) and Garrett & Cummins (2005). It continues the work with important new aspects and places it on a more solid foundation: specifically, we make implicitly made assumptions by Garrett & Cummins (2005) explicit, cf. § 2.6. We show consistency of the more general theory with previous results gained for the special case $\sigma = 1$ only, cf. §§ 2.5 and 2.6 and figure 5.

More generally, we avoid overestimating the energy yield in any case ensured by the focus on the energy equation and arrive at a concise and thus also practically applicable answer to the question of how a tidal stream can be optimally controlled by turbine arrays. We generalise the specific findings of Garrett & Cummins (2005), Pelz (2011) and Pelz *et al.* (2020). In this way, a theory and results are presented that are free of contradictions, conservative and applicable. The theory and results apply to the entire system consisting of basins I and II, the channel and the turbine array within for a complete tidal cycle.

The named conflicts in previous works become obvious by looking at one easy-to-show example for the asymptotic case $\sigma \to 1$. If such a turbine farm harvests a major part of the energy lost in the channel, a change in energy height occurs over the array. This, however, requires a water head drop and an acceleration of the downstream flow, i.e. $\alpha > 1$. The result reported by Vennell (2010*a*) that α is smaller than one for optimally tuned turbine arrangements thus contradicts the energy equation; although this conflict is easy to miss for small head differences with $\Delta H/H_I \to 0$ and $\alpha \to 1$ where the limit is approached from above, i.e. even for α being close to one it is still larger than one.

For its practical relevance, the paper develops a general and easy-to-use method for calculating the maximum power output of tidal turbines in a tidal channel or strait, which – in contrast to previous results based on Garrett & Cummins (2007) or Houlsby *et al.* (2008) – is valid for any headloss amplitudes $\Delta H = H_I - H_{II}$ for subcritical channel flow, i.e. Froude numbers $Fr < 1$, and arbitrary blockage ratio $0 < \sigma \leqslant 1$. Thereby, it forms the foundation for a physically sound optimal flow control rule.

To this end, the paper is structured as follows: in § 1.4 the underlying basis of Garrett & Cummins (2005), Pelz (2011) and Pelz *et al.* (2020) is briefly restated. In § 2.1 the variational problem for optimal flow control in general and for the special but highly relevant case of quasi-steady flow is formulated. The optimality condition for quasi-steady flow is first solved for the special case of a lossless turbine fence, discussing the results of Garrett & Cummins (2005) (§ 2.4) and showing the consistency with the works of Garrett & Cummins (2005) and Pelz (2011) (see § 2.6). The variational problem is solved second for a regular turbine fence with arbitrary blockage, whose total system efficiency for the control volume, i.e. subsystem, labelled CV 1-2 in figure 1 is derived from the generalised actuator disc model of Pelz *et al.* (2020) in § 2.7. In § 2.9 exemplary applications of the presented approach are briefly discussed, before a conclusive discussion of this work is given in § 3.

1.4. *Basis of the paper*

As depicted in the upper left of figure 2, there exists an optimal flow control rule for the complete system labelled CV I-II which is valid for the special case of full blockage $\sigma = 1$ and $\eta_T = 1$ (Garrett & Cummins 2005).

The introduced reference power for the system ranging from an upstream basin I to a downstream basin II, cf. figure 1, is given innately. It is the maximum dissipated energy

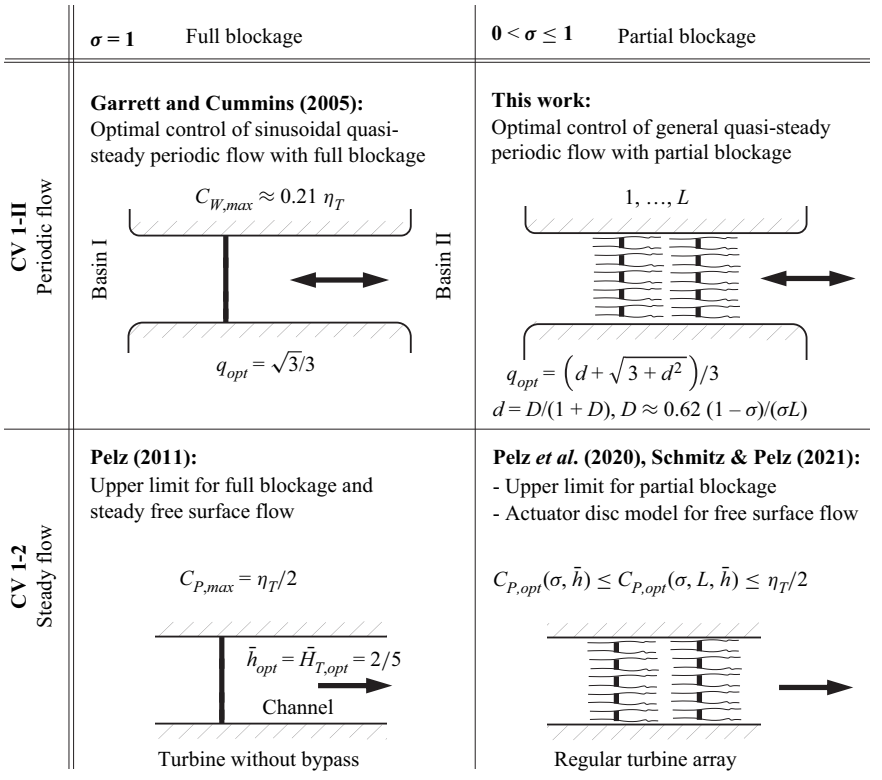

Figure 2. Classification of research on the optimal control of tidal flow and the upper limit of tidal power into periodic vs steady flow on the one hand and complete blockage vs partial blockage on the other. Only papers on which the paper presented here is based are cited in the figure.

per unit time due to the undisturbed flow between the two basins driven by the difference in energy head $\Delta H = H_I - H_{II}$: the energy equation in integral form for CV I-II (for a strict derivation of this equation from the first law of thermodynamics, see e.g. Pelz 2011) spanning from I to II without any turbine, i.e. $\sigma = 0$, gives this dissipated energy per unit time at any instant of the tidal cycle

$$\text{CV I-II}, \sigma = 0: \quad P_{D,0}(t) = \varrho g Q_0(t) \Delta H(t). \tag{1.3}$$

It should be pointed out here that $P_{D,0}$ is not only due to the flow of kinetic energy through the channel, as is sometimes reported.

As the flow in most tidal channels is quasi-steady, cf. § 2, there is usually no phase shift between the volume flow $Q(t) = Q(t+T)$ through a channel between two basins and the head difference $\Delta H(t) = \Delta H(t+T)$ between these basins (here T denotes the cycle time). In a true quasi-steady flow, this phase shift is indeed zero. This is of course not the case for the heads $H_I(t)$ and $H_{II}(t)$ of the two basins themselves. In fact, their phase difference is the reason for a cyclic head difference $\Delta H(t) = \Delta H(t+T)$ to occur. Thus, the peak values $\Delta\hat{H} = \max(\Delta H(t))$ and $\hat{Q} = \max(Q(t))$ occur at the same time and the peak dissipated power is indeed

$$\hat{P}_{D,0} = \varrho g \hat{Q}_0 \Delta\hat{H}. \tag{1.4}$$

The denominator $\hat{P}_{D,0}$ of the energy coefficient C_W, (1.6), is thus given innately, whereas the numerator is of course the total mechanical work

$$W_T = \int_0^T P_T \, \mathrm{d}t \tag{1.5}$$

extracted from the tidal flow by all turbines along a full tidal cycle divided by the cycle time T. Here, P_T is the accumulated power of all turbines. The energy coefficient is thus defined by

$$\text{CV I-II} : C_W := \frac{W_T/T}{\varrho g \hat{Q}_0 \Delta \hat{H}}. \tag{1.6}$$

For the common case of quasi-steady flow, i.e. zero time shift between head difference and volume flow rate, Garrett & Cummins (2005) derive the upper limit (see the upper left picture in figure 2)

$$\text{CV I-II}, \sigma = 1 : \; C_{W,max} = 0.21 \eta_T \quad \text{for } q_{opt} = \frac{\sqrt{3}}{3} \approx 58\,\%. \tag{1.7}$$

The turbine efficiency η_T was added by the authors to achieve a physically consistent representation. Garrett & Cummins (2005) obtained the upper limit by analysing the response of a time harmonic, i.e. sinusoidal oscillating, tidal flow through a zero-loss turbine fence. Thus, there is no dissipation due to mixing of bypass and turbine volume flow downstream of the turbine fence, i.e. $P_{D,M} = 0$. This is only true for the special case $\sigma = 1$. In addition, Garrett & Cummins (2005) assume no internal losses in the turbine's near field, i.e. $\eta_T = 1$ where the hydraulic turbine efficiency is defined as usual: $\eta_T := P_T/(P_T + P_{D,T})$. Here, P_T is the turbine power and $P_{D,T}$ is the energy dissipated in the turbine per unit time. This internal dissipation has three main contributions: (i) viscous or turbulent friction in the boundary layers of the turbine blades; (ii) losses due to wake flow of each blade section in case of partial flow separation, e.g. by boundary layer separation or also by sheet cavitation; and (iii) losses due to tip and hub vortices.

As depicted in the lower left of figure 2, there is for $\sigma = 1$ as well an upper limit for the power coefficient (1.12) for the subsystem labelled CV 1-2 in figure 1: Pelz (2011) analysed the turbine fence solely within control volume CV 1-2. The energy equation in integral form in this case reads

$$\text{CV 1-2:} \quad \varrho g Q \, (H_1 - H_2) = \frac{P_T}{\eta_T} + P_{D,M} = \frac{P_T}{\eta}. \tag{1.8}$$

Here, the total dissipation within CV 1-2, i.e. the sum of turbine internal dissipation $P_{D,T}$ and dissipation that takes place downstream of the turbine due to wake mixing $P_{D,M}$ is measured via the total system efficiency (see figure 3)

$$\eta(\sigma, q, \bar{h}) := \frac{P_T}{P_T + P_{D,T} + P_{D,M}} = \frac{\eta_T}{1 + P_{D,M}/(P_T/\eta_T)}. \tag{1.9}$$

Here, $\bar{h} := H_{II}/H_I$ is given as the boundary condition of the problem (Pelz *et al.* 2020).

For the special case of full blockage, $\sigma = 1$, the total system efficiency becomes $\eta = \eta_T$ as the mixing losses are not present, i.e. $P_{D,M} = 0$. Pelz (2011) solves the optimisation problem $\max(P_T)$ for given H_1 and width b of the tidal channel, yielding $\bar{h}_{opt} = 2/5$, $H_{T,opt} = 2/5\, H_I$. The turbine head is defined as usual by $H_T := P_T/(\eta_T \varrho g Q_T)$, where Q_T is the part of the total volume flow Q entering the turbines. In terms of volume

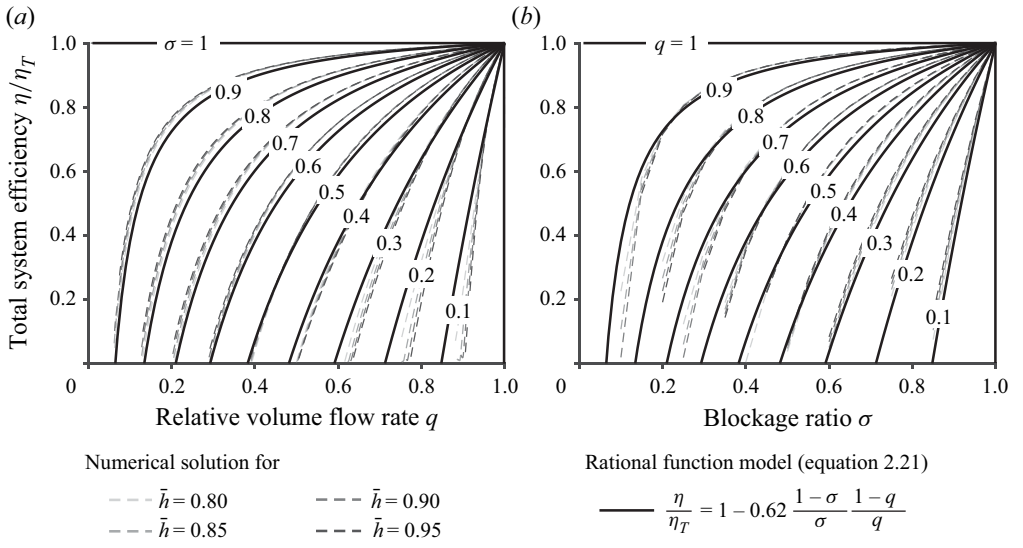

Figure 3. Total system efficiency $0 \leqslant \eta/\eta_T \leqslant 1$ vs blockage $0 < \sigma \leqslant 1$ (*a*) and relative flow rate $0 \leqslant q \leqslant 1$ (*b*) with $\bar{h} = 0.80,\ 0.85,\ 0.90,\ 0.95$ being the Coulter parameter, each close to one. The system efficiency characterises the subsystem CV 1-2 of the system CV I-II. The broken lines show (*a*) the numerical solution of the turbine disc model. The solid lines show (*b*) the analytical approximation given by (2.21).

flow, this optimality condition and the resulting upper limit writes (see the lower left picture in figure 2)

$$\text{CV 1-2, } \sigma = 1: \quad \bar{h}_{opt} = \frac{2}{5}, \quad Q_{opt} = bg^{1/2}\left(\frac{2}{5}H_I\right)^{3/2}, \quad P_{T,max} = \eta_T \varrho b g^{3/2}\left(\frac{2}{5}H_I\right)^{5/2}. \tag{1.10a–c}$$

At this optimal operation point, the first half of the tidal power is extracted within the ideal turbine fence and the second half is lost in the tailwater. Hence, the available power harvestable by a hypothetical ideal machine without tail water, $\bar{h} = 0$, is twice the above, i.e.

$$P_{avail} := 2\frac{P_{T,max}}{\eta_T} = 2\varrho b g^{3/2}\left(\frac{2}{5}H_I\right)^{5/2}, \tag{1.11}$$

for a turbine efficiency $\eta_T = 1$, cf. Pelz (2011). The upper limit of the power coefficient is therefore

$$C_{P,max} := \frac{P_{T,max}}{P_{avail}} = \frac{\eta_T}{2}. \tag{1.12}$$

Two points are worth mentioning here. First, P_{avail} cannot be obtained by applying the asymptotic limit $\bar{h} \to 0$ to the energy equation (1.8). Instead, the reference power is obtained by setting $\bar{h} = 0$. This means a change in topology, namely that in the thought experiment a machine without tailwater is considered (Pelz 2011). This corresponds to the thought experiment of Betz (1920) to determine the available reference power for a wind turbine. Second, and clearly more important in the context of this paper, we will show that the two upper limits for the power coefficient $C_{P,max} = \eta_T/2$ (1.12) on the one hand and the energy coefficient $C_{W,max} \approx 0.21\ \eta_T$ (1.7), on the other hand, are consistent.

This special case $\sigma = 1$ treated by Garrett & Cummins (2005) for CV I-II and by Pelz (2011) for CV 1-2 is, however, quite academic. A more practical question is:

> 'What energy gain is theoretically possible over a complete tidal cycle for the CV I-II system, where the blockage ratio σ may be limited by ecological and economic constraints and the volume flow ratio q may be limited by a constraint due to the flow resistance given by the drag coefficient C_D of the turbine, ensuring that the strength of the structure and mooring is greater than the stress?'

To answer this question for the subsystem CV 1-2, Pelz *et al.* (2020) consistently generalise the upper limit (1.12) for arbitrary blockage ratio $0 < \sigma \leqslant 1$ by solving the optimisation problem

$$\text{CV 1-2:} \quad C_{P,opt}(\sigma, \bar{h}) = \max_{\bar{H}_T} C_P(\sigma, \bar{H}_T, \bar{h}) \leqslant \frac{\eta_T}{2}, \tag{1.13}$$

with $\bar{H}_T := H_T/H_I$ for a regular turbine fence with $L = 1$, cf. lower right picture in figure 2.

To the best of the authors' knowledge, there is so far no analysis concerning the complete transient system covered by CV I-II, which is valid for any headloss amplitudes $\Delta H = H_I - H_{II}$ with subcritical Froude numbers $Fr < 1$ and arbitrary blockage ratio $0 < \sigma \leqslant 1$, cf. upper right of figure 2. To derive the optimal control variable, i.e. the optimal operational parameter $0 < q_{opt} \leqslant 1$ at any instant of the complete tidal cycle, $0 < t \leqslant T$, we solve the optimal control problem for the complete system

$$\text{CV I-II:} \quad \max_{q(t)} W_T = \max_{q(t)} \int_0^T P_T\left(\sigma, q(t), \bar{h}(t)\right) \mathrm{d}t, \tag{1.14}$$

for the total mechanical work extracted from the tidal flow by all turbines along a full tidal cycle as a function of the given design parameter $0 < \sigma \leqslant 1$ and given time history of the constraint $0 < \bar{h}(t) = \bar{h}(t + T) \leqslant 1$, which is given by the downstream boundary condition

$$0 < \bar{h}(t) := H_{II}(t)/H_I(t) \leqslant 1. \tag{1.15}$$

2. Optimal flow control problem

The optimisation problem (1.14) is equivalent to the variational problem

$$0 = \delta \int_0^T P_T(\sigma, q(t), \bar{h}(t), \ldots)\, \mathrm{d}t. \tag{2.1}$$

This optimal control problem is to be solved by the variational principle aiming for an optimal trajectory of the control variable $q_{opt}(t)$ for given partial blockage $0 < \sigma \leqslant 1$, i.e. the design of the fence, and arbitrary given cyclic boundary condition $\bar{h}(t) = \bar{h}(t + T)$.

The selection of the relative volume flow q (1.1) as the control variable instead of the induction factor α, as in Garrett & Cummins (2007) or Vennell (2010*a*), or the turbine head $\overline{H}_T$, as in Pelz (2011) and Pelz *et al.* (2020) has two major advantages. First, for a turbine cascade, i.e. a row of turbines arranged in flow direction, the volume flow is always the same for all turbines, whereas the turbine head differs (Schmitz & Pelz 2021). This is important for a possible generalisation of the approach presented here where one turbine fence is considered alone, in relation to turbine arrays where several turbine fences are cascaded. Second, by selecting the relative volume flow $q(t)$ as operational parameter, we can ignore the influence of $\bar{h}(t)$ on the optimal flow

control problem (2.1) as the reference volume flow $Q_0(t)$ results from the upstream and downstream boundary condition, i.e. $H_1/H_I = 1$ and $\bar{h} = H_{II}/H_I$. In other words, q depends on the boundary condition $\bar{h}$ and the design parameter σ only. Hence, for a given design parameter σ, the variational problem (2.1) reads

$$0 = \delta \int_0^T P_T\left(q(t), \dot{q}(t)\right) \mathrm{d}t, \tag{2.2}$$

where $\dot{q} = \mathrm{d}q/\mathrm{d}t$ is the time derivative of the operational parameter (1.1). This variational problem (2.2) is equivalent to the Euler–Lagrange equation

$$\frac{\mathrm{d}}{\mathrm{d}t}\left(\frac{\partial P_T}{\partial \dot{q}}\right) = \frac{\partial P_T}{\partial q}. \tag{2.3}$$

2.1. *Optimality condition for quasi-steady flow*

For a quasi-steady problem, all terms with partial time derivatives in the continuity equation, the momentum equation and the energy equation are negligibly small and time enters the problem only as a parameter in the boundary conditions: $H_1(t) = H_I(t)$ and $h_2(t) = H_{II}(t)$. If this is the case, the left-hand side of (2.3) is negligibly small and the optimisation problem assumes the most-simple form

$$\frac{\partial P_T}{\partial q} = 0. \tag{2.4}$$

There are three conditions that must be fulfilled in order to qualify a channel flow as quasi-steady, as outlined in Appendix A,

$$\left.\begin{aligned} \Pi_1 := f\sqrt{LC} = \frac{fl}{\sqrt{gh_0}} \ll 1, \quad \Pi_2 := \frac{fL}{R} = \frac{fh_0}{u_*} \ll 1, \\ \Pi_3 = \frac{\Pi_1^2}{\Pi_2} = fRC = \frac{fu_*}{g}\left(\frac{l}{h_0}\right)^2 \ll 1. \end{aligned}\right\} \tag{2.5a–c}$$

Here, the capacitance C, inductance L and resistance R are used for the electrical analogue of the flow, cf. figure 1 and Appendix A. The three conditions can be derived by an order of magnitude analysis of the equations of motion (Pelz, Lemmer & Schmitz 2022) or by an extended dimensional analysis, as is presented in the Appendix A.

With the frequency of the tidal cycle $f = 1/T \sim 10^{-4}$ Hz, the undisturbed water depth $h_0 \sim (10^1 \ldots 10^2)$ m, the typical length range of tidal channels $l \sim (10^3 \ldots 10^4)$ m and the typical frictional velocity (see Appendix A) $u_* \sim (0.2 \ldots 0.3)$ ms^{-1} the three dimensionless products show a magnitude of $10^{-3} \ldots 10^{-1}$. Therefore, the necessary conditions for the quasi-steady flow are fulfilled for the vast majority of tidal channels. Only for very long and shallow channels, transient effects become relevant. The turbulent diffusion time u_*/h_0 can only have an effect for very deep channels.

In fact, it would be valuable information to represent the large number of narrow channels or straits between two basins that are considered to be suitable for tidal power plants on Earth in three diagrams and evaluate them in terms of their dynamic properties. This would mean that that the dimensionless products of the channels are plotted in three diagrams, i.e. Π_2 vs Π_1, Π_3 vs Π_1 and Π_3 vs Π_2, each in a range of values between zero and one. Each diagram would be the projection of a unit cube. The so far publicly available data are still so rare and incomplete that this representation cannot be given in

this paper. The aim of the work is a scientific analysis and a consistent method. However, the relevance of the work naturally increases with its applicability. Based on the available data and using the estimation of the dimensionless products made above, we can only assume in the context of this work that most channels are so 'short' that the flow is indeed quasi-steady.

For quasi-steady flow, (2.4) leads us to the optimal control of the quasi-steady flow and thus to the amount of tidal power achievable by an optimally operated turbine fence or array with partial blockage over the entire tidal cycle.

2.2. *Transient channel flow*

Although a channel flow unaffected by a turbine can be quasi-steady, it can still be set to a transient state by latching the turbine in one time phase and allowing it to operate in the following time phase. This so-called latching control strategy known in the field of wave power is discussed by Vennell & Adcock (2013) and Vennell (2016) for tidal channels.

The approach from Vennell (2016) is very interesting and promising from our point of view: it is common knowledge that the potential for extracting mechanical energy from a dynamically oscillating system such as a wave point absorber with natural frequency $1/\sqrt{LC}$, which interacts with waves of frequency f, reaches its maximum at resonance, i.e. for $f\sqrt{LC} \approx 1$. Usually, the eigenfrequency of the unit is much higher than the excitation frequency from wave (or tide) due to technical limitations, i.e. $f\sqrt{LC} \ll 1$ as is the case with many tidal channels. By applying the latching control strategy, the system can be forced to behave as if $f\sqrt{LC} \approx 1$, i.e. it is forced to behave dynamically and to approach resonance. For the dynamic and hence transient case, the left-hand side of the Euler–Lagrange equation (2.3) is different from zero. Although this is a promising strategy to improve the energy yield, it is not the focus of this paper. Here, we only consider continuously operated turbines whose operating point is determined by $q(t)$.

2.3. *General solution for quasi-steady flow*

In order to find a general solution to (2.4), it is useful to apply a suitable reference power. As stated earlier, Garrett & Cummins (2005) and Black & Veatch Consulting Ltd (2005) define the peak power $\hat{P}_{D,0}$ given by (1.4) as a reference. As this paper shows, it is more beneficial to use the dissipated energy for the undisturbed channel at every instant in time of the tidal cycle $P_{D,0}(t) = \varrho g Q_0(t)\Delta H(t)$ (1.3) as a reference.

In addition to the energy equation formulated for the system labelled by CV I-II in figure 1 without turbines, cf. (1.3), we consider the energy equation formulated for the same system with turbines installed

$$\text{CV I-II}, 0 < \sigma \leqslant 1: \quad \varrho g Q \Delta H = \frac{P_T}{\eta_T} + P_{D,M} + P_D = \frac{P_T}{\eta} + P_D. \tag{2.6}$$

The upstream boundary condition of the energy equation is energetic, the downstream boundary condition dynamic. A kinematic boundary condition is often used upstream of turbine fences and arrays. However, it has been shown that this kinematic boundary condition, which follows the theory of wind turbines, is misleading, cf. Pelz *et al.* (2020, 2022). Upstream, the hydraulic grade line is level due to usually negligible dissipation for an accelerated flow. Hence, the upstream boundary condition is $H_1/H_I = 1$ with the total head defined by $H := z + h + u^2/2g$. Here, z is the level of the seabed, $u = Q/(bh)$ is the flow velocity averaged over the cross-section and h is the

water depth. For the purposes of this paper, we assume a levelled seabed within the tidal channel. The downstream boundary condition is given by the ratio of downstream water depth to effective head, $\bar{h} := h_2/H_I$. For subcritical flow, i.e. $Fr_2 < 1$, Newton's third law '*actio est reactio*' for the tidal stream entering the lower basin gives $h_2 = H_{II}$. Hence, the cyclic downstream boundary condition reads $0 < \bar{h}(t) := H_{II}(t)/H_I(t) \leqslant 1$. For $\bar{h} = 1$ there is no channel flow. For $\bar{h} < 1$ the flow is from left to right (see figure 1). For $\bar{h} > 1$ the flow is from right to left which is covered by switching the indices $I \to II$, $II \to I$, $1 \to 2$ and $2 \to 1$. Hence, it is sufficient to analyse the interval $0 < \bar{h} \leqslant 1$ only. For real tidal channel flow, $\bar{h}$ is close to one and Fr_2 is much smaller than one. We will use this fact in § 2.7 to give a concise analytical approximation to the numerical solution of the physically consistent actuator disk model Pelz *et al.* (2020) with (2.21).

To account for dissipation due to fluid friction at the seabed, we define a loss factor $\zeta := c_f l/h_0$ with the seabed friction factor c_f. Thus, we obtain for the dissipation powers for the disturbed and undisturbed tidal channel

$$P_D = \frac{1+\zeta}{2}\varrho\frac{Q^3}{b^2h_2^2}, \quad P_{D,0} = \frac{1+\zeta}{2}\varrho\frac{Q_0^3}{b^2h_{2,0}^2}. \tag{2.7a,b}$$

There might be a discussion regarding modelling the loss factor ζ. Interestingly, however, this is not necessary, since the results are independent of the loss model. This is true provided the following assumptions hold. First, viscous shear stress is small compared with turbulent stress and, second, no hydraulic jump or surge wave occurs. Both assumptions are true for most marine open channel flow; there is no hydraulic jump in subcritical flow to reflect the latter concern. In addition, the viscous shear stress is generally negligible because the viscous sublayer usually 'disappears' in the roughness of the seabed, i.e. $k \gg \nu/u_*$. Hence, $P_D \propto Q^3$ and the downstream water depth in (2.7*a*,*b*) is given by the boundary condition $h_2(t) = h_{2,0}(t) = H_{II}(t)$ for both cases, i.e. $\sigma = 0$ and $0 < \sigma \leqslant 1$ respectively. In the framework of the optimisation, the dissipation due to friction at the channel bottom and at the exit of the channel flow into the basin is proportional to the resistance constant R and proportional to Q^3. The resistance constant is only parametrically dependent on time via the boundary condition, i.e. the water depth $h_2 = H_{II}$, which is typical for quasi-steady flows

$$R := \frac{1+\zeta}{2}\frac{\varrho}{b^2H_{II}^2}. \tag{2.8}$$

Hence, (2.7*a*,*b*) read $P_D = RQ^3$ and $P_{D,0} = RQ_0^3$, keeping in mind that $R(t) = R(t+T)$ since $H_{II}(t) = H_{II}(t+T)$. With the total system efficiency (1.9) and the abbreviation (2.8) the energy equations (2.6) and (2.7*a*,*b*) read

$$\sigma \neq 0: \quad \varrho g Q \Delta H = \frac{P_T}{\eta} + RQ^3 \quad \text{and} \quad \sigma = 0: \quad \varrho g Q_0 \Delta H = RQ_0^3 = P_{D,0}. \tag{2.9a,b}$$

Besides the analysis of the special case $\sigma = 1$ and sinusoidal periodic flow in § 2.6 we are only bounded by relative quantities such as the relative volumetric flow $q := Q/Q_0$ and the relative turbine power p defined by $p := P_T/P_{D,0}$. Hence, the details of any loss model like friction on the seabed ground is only of minor relevance. The combination of the two energy equations (2.9*a*,*b*) using the definitions for q and p results in the surprisingly concise equation

$$p = \eta(\sigma, q)q(1-q^2), \tag{2.10}$$

which is still an energy equation in integral form for the control volume CV I-II with the turbines' power output on the left-hand side.

To obtain the optimal power output at every instant in time along the tidal cycle and the maximum of work per cycle

$$\max \int_0^T \eta q(1-q^2)\,\mathrm{d}t, \tag{2.11}$$

we solve the special form of the Euler–Lagrange equation for quasi-steady flow (2.4). As the system efficiency $\eta = \eta(\sigma, q)$ does depend on the relative volume flow q, this yields

$$-\frac{1}{\eta}\frac{\partial \eta}{\partial q} q(1-q^2) = 1 - 3q^2. \tag{2.12}$$

This optimality condition for deriving the optimal trajectory of the relative volume flow $q_{opt}(t)$ applies to any periodic but quasi-steady flow in the tidal channel for any turbine array.

2.4. *Optimal flow control for full blockage* $\sigma = 1$

Before determining the slope $(\partial\eta/\partial q)/\eta$, using the generalised actuator disc model for free surface flow by Pelz *et al.* (2020), we first treat the simple and special case of full blockage $\sigma = 1$ and $\eta = \eta_T$ = const. For this case, the left-hand side of (2.12) vanishes as $\partial\eta/\partial q = 0$. Hence, (2.12) yields the special result of Garrett & Cummins (2005), i.e.

$$\sigma = 1: \quad q_{opt} = \frac{\sqrt{3}}{3} \approx 0.58. \tag{2.13}$$

Using this result in (2.10), we gain the result for the maximal relative power

$$p_{max} = \frac{2\sqrt{3}}{9}\eta_T \approx 0.39\eta_T. \tag{2.14}$$

This analytic result in form of a fractional irrational number is new and not given by Garrett & Cummins (2005). With the track based on optimal control theory and making the implicitly made assumptions explicit, cf. § 2.6, the theory of Garrett & Cummins (2005) is put on an even more solid basis.

2.5. *Consistency with Pelz (2011) for quasi-steady flow and* $\sigma = 1$

The upper limit (2.14) is consistent with the upper limit (1.12) of Pelz (2011), as the following analysis shows: The difference in the reference power $P_{D,0} := \varrho g Q_0 \Delta H$ used in this paper and $P_{avail} := 2\varrho b g^{3/2}(2/5H_I)^{5/2}$ defined by Pelz (2011) is due to the difference in the considered systems. That is, they serve different purposes and are as such complementary, but consistent. This becomes obvious by inserting the result (2.14) into the upper limit for the power coefficient (1.12) yielding

$$C_{P,max} = \frac{P_{T,max}}{P_{avail}} = \eta_T \frac{\sqrt{3}}{9} \frac{Q_0 \Delta H}{b g^{1/2}(2/5H_I)^{5/2}}. \tag{2.15}$$

With $\Delta H = H_I\,(1-\bar{h})$ and the optimal operation point $Q_{opt} = b g^{1/2}\,(2/5H_I)^{3/2}$, $\bar{h}_{opt} = 2/5$ (1.10*a–c*) derived by Pelz (2011), as well as the optimal operation $Q_{opt} = Q_0/\sqrt{3}$ (2.14) derived in this paper, (2.15) collapses into

$$C_{P,max} = \frac{\eta_T}{2}. \tag{2.16}$$

This is indeed the upper limit (1.12) for the power output out of any quasi-steady free surface flow (Pelz 2011; Pelz *et al.* 2020).

2.6. *Consistency with Garrett & Cummins (2005) for harmonic flow and* $\sigma = 1$

The analyses and results presented so far apply to any cyclic but quasi-steady flow. Garrett & Cummins (2005) considered a special case by assuming two things in deriving their upper bound for the energy coefficient (1.7). First, the authors assume a harmonic, i.e. sinusoidal, flow. Second, they assume that the flow resistance $R(t) \approx R_c$ is approximately constant without considering the time variation that actually exists (see (2.8)).

Although both assumptions are not necessary as this paper shows, only in this section do we make these very assumptions to show that the analysis presented here is consistent with that of Garrett & Cummins (2005) and, moreover, a generalisation of it.

For this special case, we have $\Delta H(t) = \Delta\hat{H}\sin(\Omega t)$, $\Omega = 2\pi f = 2\pi/T$. With $R \approx R_c = \text{const.}$ (2.9*a*,*b*) yields

$$Q_0 = \sqrt{\frac{\varrho g \Delta H}{R}} \approx \hat{Q}_0 \sqrt{\sin(\Omega t)} \tag{2.17}$$

with the peak volume flow rate $\hat{Q}_0 = \sqrt{\varrho g \Delta\hat{H}/R_c}$. The dissipated energy per unit time in the undisturbed channel is hence given by the approximation

$$P_{D,0} \approx \hat{P}_{D,0} \sin^{3/2}(\Omega t), \tag{2.18}$$

with the peak power $\hat{P}_{D,0} = \varrho g \hat{Q}_0 \Delta\hat{H}$ already given in (1.4).

With the result $P_{T,max} = \eta_T 2\sqrt{3}/9\, P_{D,0}$ (2.14), the time averaged maximal power output for $\sigma = 1$ thus calculates as

$$C_{W,max} = \frac{1}{2\pi}\int_0^{2\pi} \frac{P_{T,max}}{\hat{P}_{D,0}}\,\mathrm{d}(\Omega t) = \eta_T \frac{2\sqrt{3}}{9}\, c \approx 0.21\eta_T, \tag{2.19}$$

with the conversion factor c between the relative turbine power p used in this paper and the energy coefficient C_W usually used for resource characterisation of tidal power

$$c := \frac{C_W}{p} \approx \frac{1}{2\pi}\int_0^{2\pi} |\sin^{3/2}(\Omega t)|\,\mathrm{d}(\Omega t) \approx 0.56. \tag{2.20}$$

(It is clear that with non-harmonic tidal flow, the conversion factor takes on a different value. This can be easily calculated for any measured time cycle.)

Equation (2.19) is indeed the upper limit given by Garrett & Cummins (2005).

For quasi-steady flow, the results and methods presented in the previous sections are thus a consistent generalisation of the special harmonic case treated by Garrett & Cummins (2005). As this paper shows, neither the consideration of sinusoidal flow, nor the approximation of a time-invariant $R = R_c$ is necessary when having p and not C_W as objective.

So far, the consistency of the optimal control approach has been proven for the special case $\sigma = 1$. The following section closes the knowledge gap for the arbitrary blockage ratio $0 < \sigma \leqslant 1$.

2.7. *Optimal flow control for a regular turbine fence with partial blockage* $0 < \sigma \leqslant 1$

The present section fills the mentioned knowledge gap by (*a*) solving the model of the turbine disk numerically in conjunction with the Euler–Lagrange equation which covers the entire time-periodic system CV I-II and (*b*) solving the problem analytically using an approximation of the turbine properties. Thereby, the analytical solution (*b*) is

validated against the numerical solution (a). The validation shows only a very small model uncertainty in the relevant parameter range. It is also surprisingly concise and easy to use in practice, as we will show with the help of use cases, cf. § 2.9.

The approach based on the Euler–Lagrange equation derived in § 2.1 provides a rigorous and consistent way to generalise the results presented in the previous section for full blockage $\sigma = 1$ for arbitrary, i.e. also partial blockage (see (2.12)). To solve the optimality condition (2.12) the total system efficiency η and its slope $-(\partial\eta/\partial q)/\eta$ has to be determined for arbitrary blockage $0 < \sigma < 1$, volume flow q and boundary condition $\bar{h}$. This is done using the axiomatic and physically consistent turbine fence model of Pelz *et al.* (2020).

Figure 3 shows the total system efficiency η/η_T for $0 < \sigma \leqslant 1$ and $0 < q \leqslant 1$ for the subsystem CV 1-2 derived from the turbine disc model of Pelz *et al.* (2020). The dashed lines show (a) the numerical results of the turbine disc model being valid for free surface flow. The Coulter parameter in the two plots shown in figure 3 is the basin head ratio $\bar{h} = 0.80,\ 0.85,\ 0.90,\ 0.95$.

The solid lines represent (b) the analytical approximations of the numerical results. The basis for the approximation is the following analysis: For $\sigma \to 1$ we have the asymptotic behaviour $\eta \to \eta_T$ as no mixing occurs. The same is true for the limit $q \to 1 : \eta \to \eta_T$, where the resistance and hence the mixing losses disappear. Operating the turbines at increased resistances results in a decreased turbine volume flow and increased energy loss due to mixing in the wake. In the theoretical limit of maximum resistance, i.e. a closed disc, there is no turbine volume flow. All the volume flow is bypassed and all power is dissipated in the turbine wake, i.e. $\eta \to 0$. This gives the monotonic behaviour, which is revealed in figure 3. Further, there is only a negligible sensitivity of η/η_T with respect to $\bar{h}$. This is true at least for the practically relevant range where $\bar{h}$ is close to one. This is because the main dependence on $\bar{h}$ is already covered by $q = q(\bar{h})$. The total efficiency of the system η is therefore only implicitly dependent on $\bar{h}$, but only to a small extent explicitly: $\eta(q, \bar{h}, \sigma) \approx \eta(q(\bar{h}), \sigma)$.

The asymptotes, the monotonicity and the implicit dependence of the total system efficiency on $\bar{h}$ suggest a rational ansatz function (b) for the approximation. Indeed, the numerical solution (a) of the turbine model yielding the total system efficiency can be approximated by a rational ansatz function (b) mapping the limiting characteristics for $\sigma \to 1$ and $q \to 1$. An analytical approximation to the numerical values is given by the rational function

$$\frac{\eta}{\eta_T} \approx 1 - a\frac{1-\sigma}{\sigma}\,\frac{1-q}{q}. \tag{2.21}$$

Here, the second quotient $(1-q)/q$ is an 'operating' function, whereas the first quotient is a 'design' function of the regular turbine array. In the following we will use the abbreviation for this first quotient defined by

$$D(\sigma) := a\frac{1-\sigma}{\sigma}. \tag{2.22}$$

For a single regular turbine fence, the constant a is determined by means of a Gaussian root means square method to be $a \approx 0.62$. In the context of this paper, we focus on one single turbine fence $L = 1$ in a tidal channel only.

Provided the turbine fence is extended to a turbine array in which $L = 1, 2, \ldots$ turbine fences are arranged in a cascade, it is conjectured that a will be a function of this additional parameter which, along with σ, defines the design of the ideal turbine array. In fact, our current research on turbine arrays shows that the rational design function is then given by

$D(\sigma, L) = (a/L)\,(1-\sigma)/\sigma$ for an ideal turbine array spanning the entire width b of the tidal channel. For $L = 1$, the special case of an ideal turbine fence (2.22) is part of this general design function. For $L \to \infty$ the design function becomes zero and $\eta \to \eta_T$ as for the special case $\sigma = 1$. The asymptotic behaviour is thus correctly reproduced by the approach taken.

In the following, the importance of the system efficiency of the subsystem CV 1-2 for the overall system CV I-II and the admissibility and simplicity of the approach will be discussed: First of all, the approach (b) is an approximation only to the turbine characteristics given by numerical model solution (a) in the relevant parameter space as turbine efficiency for subsystem CV 1-2, cf. figure 3. However, the relevant physical information about the subsystem CV 1-2 for the overall system CV-I-II, which is the focus here, is completely contained in figure 3. Thus, all independent parameters for design, considered by σ, operation, determined by q, and boundary condition, given by $\bar{h}$, are also included. The information used for CV I-II in this work is the system efficiency of the subsystem CV 1-2, which is always less than one. This ensures the consistency with the conservation of energy. It is given implicitly from the first in the new approach presented here. This would not necessarily be the case if the information from the subsystem CV 1-2 for the overall system CV I-II were a turbine's drag coefficient, as in the approaches that can be found in the reviewed literature: as already stated, up to now momentum and forces have practically always been discussed first and only energy and dissipation second. In the new approach presented here, this order is reversed, resulting in an indubitable consistency.

The prerequisite for the obvious simplicity and quality, i.e. small model uncertainty, of the approximation (b) is the careful choice of the independent variables, namely the relative volume flow q as operational parameter and the relative blockage σ as design parameter, as well as the natural restriction of the efficiency to the range of values between zero and one. The discussion of the monotonic behaviour, the asymptotic behaviour towards one and the zeros was also helpful. The validity of the approximation is obvious throughout the paper, cf. figures 3, 4 and 5. The discussion reveals that the approximation is more than just an ad hoc approach, as one might assume from its surprising simplicity. The simplicity only becomes apparent through the energy approach, the careful choice of variables and their reference values.

Using (2.21) and (2.22) the energy equation (2.10) yields

$$\frac{p}{\eta_T} = -(1+D)q^3 + Dq^2 + (1+D)q - D. \tag{2.23}$$

For $\sigma \neq 1$ this equation can be represented by the even simpler form

$$\frac{p}{\eta_T} = Dd(q-d)(1-q^2), \tag{2.24}$$

by using the abbreviation

$$d := \frac{D}{1+D}. \tag{2.25}$$

For $\sigma \to 1$ the design functions D, d both become zero and hence p would vanish in the more special form (2.24). However, the special case $\sigma = 1$ is already covered. For brevity and clarity, however, we prefer the given simple representation. Equation (2.24) has two positive roots, namely $q = 1$ and $q = d$. The first root is clear, the second root is due to the fact that for $q = d$ there is no turbine volume flow and only a bypass volume flow.

The approximation of the sweet points is gained by applying the optimal flow control condition (2.12), i.e. $\partial p/\partial q = 0$, to the approximation (2.23) or (2.24), which yields the

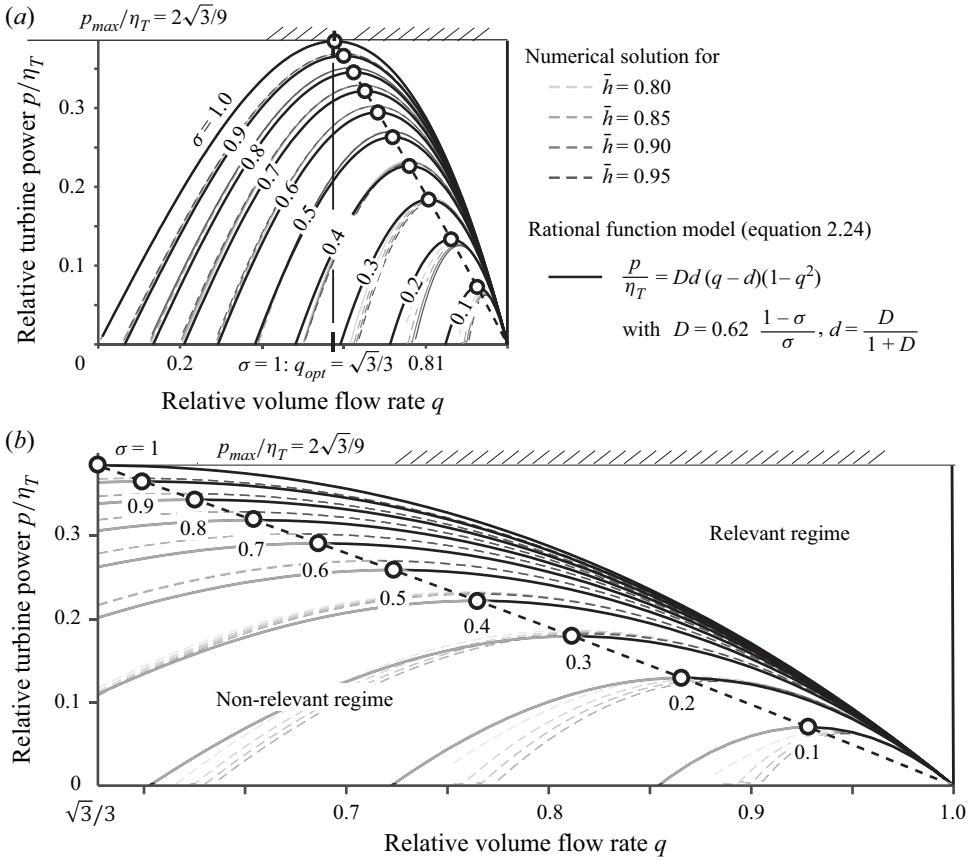

Figure 4. Relative turbine power vs relative volume flow for different blockage ratios $\sigma = 0.1, 0.2, 0.3, \ldots, 1.0$ and boundary condition $\bar{h} = 0.80, 0.85, 0.90, 0.95$. Panel (*a*) shows the whole range of relative volume flow, whereas (*b*) highlights only the relevant parameter range. The thin broken lines represent (*a*) the numerical results derived from the turbine disc model, whereas the thick solid lines represent (*b*) the rational function model given by (2.24).

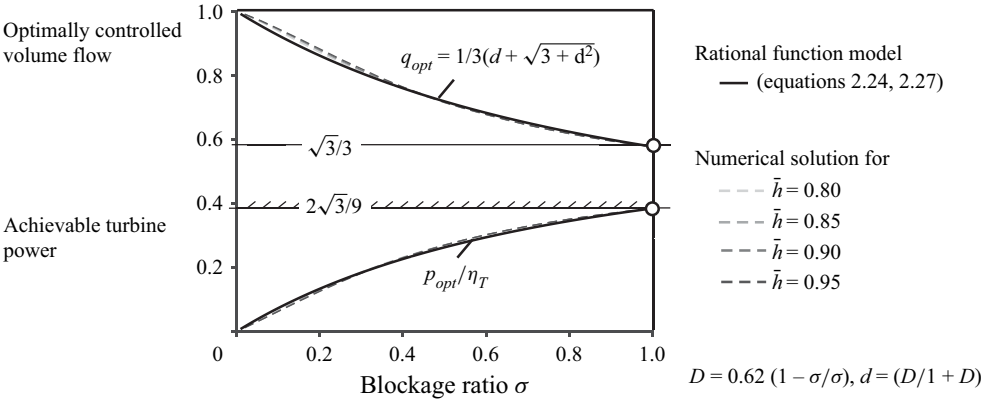

Figure 5. Optimal relative volume flow q_{opt} as well as the associated and achievable relative turbine power p as a function of blockage of the turbine fence; the thin dashed lines represent the numerical solution (*a*) based on the turbine disc model, the thick solid lines represent the rational function model (*b*) given by (2.21) and (2.22).

quadratic equation

$$3q_{opt}^2 - 2dq_{opt} - 1 = 0, \tag{2.26}$$

for the optimal relative volume flow to be controlled by the operator of the turbine array. The one relevant root of this (2.26) is given by the concise equation

$$q_{opt} = \tfrac{1}{3}(d + \sqrt{3 + d^2}). \tag{2.27}$$

For the special case $\sigma = 1$ and thus $D = d = 0$, the new solutions collapse into the familiar condition $q_{opt} = \sqrt{3}/3$, cf. (2.13), as it should be for consistency.

The strength of the analytical approach using a rational function model is revealed in figure 4. Figure 4(*a*) shows the relative turbine power $p(\sigma, q, \bar{h})$ with $0 < q \leqslant 1$ as abscissa and σ as the Coulter parameter. Figure 4(*b*) zooms into the relevant range $\sqrt{3}/3 < q \leqslant 1$ with relative volume flow higher than the optimum for $\sigma = 1$, as turbine arrays are usually operated at an operating point given by $q \geqslant q_{opt}$, as will be seen in the case studies presented in § 2.9. The non-relevant regime $q < q_{opt}$ is greyed out accordingly.

The thin broken lines present the numerical solution (*a*) of the axiomatic and for free surface flow generalised actuator disc model by Pelz *et al.* (2020) for various blockages $\sigma = 0.1, 0.2, \ldots, 1$ and boundary conditions $\bar{h} = 0.80, 0.85, 0.90, 0.95$. The thick solid lines represent the rational function (2.24), i.e. representing the analytical approach (*b*).

The sweet points fulfilling the optimality condition given by the Euler–Lagrange equation (2.12) are marked by white circles in figure 4. The root-mean-square error of the approximation is 8/1000, resulting in a model uncertainty of less than 2 % for $|\bar{h}| \geq 0.8$. This uncertainty is due to an under-prediction of the relative volume flow q for low blockages $\sigma < 0.3$ within the non-relevant regime $q < q_{opt}$ and a slight over-prediction of the relative power output p/η_T for medium blockages $0.5 < \sigma < 0.8$. For the relevant regime $q \geqslant q_{opt}$, the approximation of the rational function model is remarkably good, as depicted in figure 4(*b*).

Figure 5 gives the collection of the sweet spots marked in figure 4 by circles, i.e. the optimal relative volume and the associated achievable relative turbine power being both only a function of blockage σ. For $\sigma = 1$, the plot shows the result of Pelz (2011) and the matching approximation of Garrett & Cummins (2005). The thick solid lines represent the optimal relative flow rate (2.27) and the associated achievable turbine power. The thin broken lines represent the numerical solution of the model by Pelz *et al.* (2020).

The result presented in figure 5 is surprisingly concise: For any $Q_0(t)$ and any σ, the maximum energy yield and the necessary optimum relative flow rate are given with the result. This applies to the complete tidal cycle. The result is of practical importance for the optimal control problem that is not constrained by a bearable drag force of the turbine fence and its mooring. The constrained optimal control problem for cases limited by a maximum bearable drag force is treated in the following section, § 2.8.

The quantitative comparison with other works was possible for Pelz *et al.* (2020) when considering the subsystem CV 1-2. Unfortunately, it is not yet possible to make a meaningful comparison of the results obtained here with literature data for the CV I-II system. The difficulties are due to the fact that channels were often considered in which the flow was actually transient and not quasi-steady. This applies, for example, to Vennell (2016). Instead of making a comparison, we point to the consistency of the new results with older more specific results for $\sigma = 1$ and to the fact that the complete model is free of contradictions avoiding an overestimation of energy yield which is confirmed by experiments, at least for the model of the turbine disc forming the basis of this work.

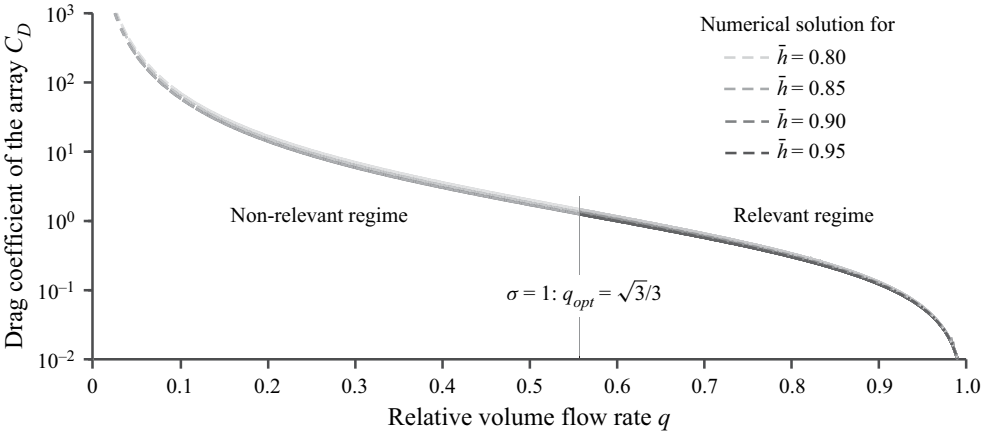

Figure 6. Required drag coefficient C_D to reach the relative volume flow q with the associated achievable relative turbine power p given by the numerical solution based on the experimental validated turbine model by Pelz *et al.* (2020); for the curves shown dissipation due to friction at the channel ground is assumed to be small relative to the Carnot loss at the channel exit.

2.8. *Constraint due to the bearable turbine drag force*

The marked sweet spots in figure 4 and the collected sweet points shown in figure 5 presuppose that the turbines and their mooring bear the required drag force F_D on all turbines of one turbine fence to reach the optimal specific volume flow rate q_{opt} and extract the associated and achievable turbine power p_{opt}. This raises the question of the relation between required and bearable force on the turbine fence. This section answers this important question from a practical point of view. From a mathematical point of view, the optimal control problem is complemented by a constraint due to the drag force that can be withstood by the turbine fence and its mooring.

The drag is represented by the drag coefficient, i.e. drag force F_D on the turbine fence non-dimensionalised with the upstream cross-sectional area A_1 and flow speed u_1

$$C_D := \frac{F_D}{\varrho A_1 u_1^2}, \tag{2.28}$$

whereby the often used factor 2 has been omitted here for reasons of conciseness. If the turbine fence is formed by K turbines, then of course the force on one turbine is F_D/K.

Figure 6 shows the required drag coefficient C_D for all $\sigma = 0.1, 0.2, \ldots, 1$ and $\bar{h} = 0.80, 0.85, 0.90, 0.95$ from figures 4 and 5, which was determined by numerically solving the turbine disk model for the subsystem CV 1-2.

As already mentioned, the drag and the associated drag coefficient is a result of the theory presented here and not an input as in previous works by other authors. The output shown in figure 6 is for a generic channel neglecting dissipation due to turbulent shear stress near the channel ground, i.e. $\zeta = 0$ (2.7*a*,*b*) and (2.8). Thus, the only loss considered for this part of the study is the Carnot loss at the channel exit and the energy loss due to mixing. In fact, the dissipation due to fluid friction at the seabed is often much smaller than mixing or Carnot losses.

As figure 6 shows, the necessary drag coefficient C_D is independent of the blockage ratio σ and furthermore only marginally dependent on the boundary condition $\bar{h}$ for the named reasons.

The practical value of figure 6 is obvious: in most practical situations, the drag coefficient is constrained by an upper bound, $C_{D,max}$, due to the bearable load. With $C_{D,max}$ as input, figure 6 gives the bearable volume flow: $q_{max} = q(C_{D,max})$. Hence, only the parameter interval $\sqrt{3}/3 \leqslant q_{max} \leqslant 0$ is of practical relevance for the conceptional design and operation of a turbine array. This is the reason why we focused on this interval in figures 4 and 6. The regimes in light grey on the left side of the two figures are practically irrelevant.

In order to enhance the applicable drag for a given blockage ratio σ, multiple turbine fences may be cascaded to a turbine array, i.e. $L > 1$. As stated earlier, this can be considered by adapting the rational design function to $D(\sigma, L) = (a/L)(1-\sigma)/\sigma$.

The results so far are summarised by three points. First, the results presented are a consistent generalisation of the results by Garrett & Cummins (2005) and Pelz *et al.* (2020) for arbitrary blockage ratios $0 < \sigma \leqslant 1$, for the full tidal cycle $0 < t \leqslant T$ and for the complete system CV I-II. Second, the overall efficiency of the system can be advantageously approximated by a rational ansatz function. Both (*a*) the numerical solution of the optimal control problem and (*b*) the analytical approximation result in a concise method. This allows to derive the optimal turbine power p_{opt} and the associated optimal volume flow q_{opt} as a function of any blockage ratio σ. The results are revealed in figure 5 and (2.27), (2.24). Third, if for technical reasons the drag force is limited, figure 6 gives the necessary mapping $\sqrt{3}/3 \leqslant q_{max} = q(C_{D,max}) \leqslant 0$.

Due to the conciseness of the representation, the results can easily be used for initial resource estimates of tidal power, as shown in the following section.

2.9. *Application of the optimal control flow rule for three typical use cases*

The paper's findings may be used to analyse the optimality of design σ and operation q under different constraints and objectives. This is shown in the following by exemplarily using the data $q \geqslant 0.9$ and $C_W = 8.6\,\%$ from the report of Black & Veatch Consulting Ltd (2005). Appendix B provides a calculation flow diagram for the blockage-dependent power potential estimation.

In the following we consider three use cases (i), (ii) and (iii). In the first use case (i) we calculate the optimal blockage for the given volume flow reduction of $q = 0.9$. For this fixed operational parameter, (2.27), (2.25) and (2.22) yield the optimal design parameter of the turbine fence $\sigma_{opt} = 0.13$. For this combination of design and operation, the turbines are operated at their maximum possible power output and thus in the most economical manner

$$\text{Use case (i):} \quad q = q_{opt} = 0.9 \rightarrow \sigma_{opt} = 0.13, \quad \frac{C_{W,max}}{\eta_T} = 5.0\,\%, \quad \frac{p_{max}}{\eta_T} = 8.9\,\%. \tag{2.29}$$

This corresponds to only approximately 60 % of the expected output of tidal stream sites (Black & Veatch Consulting Ltd 2005) even for ideal turbines with an efficiency $\eta_T = 1$, provided that, first, only turbine fences but no turbine arrays are installed and, second, that the turbine fences are optimally designed and operated.

The second use case (ii) is a turbine fence not operating at its optimum, while assuming $C_W = 8.6\,\%$ and $q = 0.9$ are both constraints of the system design. This means that the optimality condition is relaxed and q will be larger than the optimal volume flow, i.e. $q > q_{opt}$. In this set-up, $C_W/\eta_T = 8.6\,\%$ yields the constraint $p/\eta_T = C_W/(c\eta_T) = 15\,\%$. From figure 4 or equivalently from (2.24), we derive a required blockage to reach this

target of $\sigma = 0.43$ for a single turbine fence, which is quite ambitious but theoretically doable in terms of technology and ecology. For a turbine array, the required turbine area is even higher

$$\text{Use case (ii):} \quad q = 0.9, \quad \frac{C_W}{\eta_T} = 8.6\,\%, \quad \frac{p}{\eta_T} = 15\,\% \rightarrow \sigma = 0.43. \tag{2.30}$$

The third and last use case (iii) shall be the following. The first and second use case reveal that $C_W/\eta_T = 8.6\,\%$ is very ambitious, with a constraint volume flow of 90 %. In this last use case, we have the prospected power output of $C_W/\eta_T = 8.6\,\%$, $p/\eta_T = 15\,\%$ as a constraint and look for an optimal control of the tidal flow as well as for the optimal design of the turbine fence regarding the blockage ratio. From figure 4 or the presented model based on rational functions we derive $q_{opt} = 0.86$ and $\sigma_{opt} = 0.23$, i.e.

$$\text{Use case (iii):} \quad \frac{C_W}{\eta_T} = 8.6\,\%, \quad \frac{p}{\eta_T} = 15\,\% \rightarrow q_{opt} = 0.86, \quad \sigma_{opt} = 0.23. \tag{2.31}$$

Of course these values have to be ecologically and economically assessed. The three cases, however, indicate how the result of the paper can be used for resource assessment using different constraints and objectives.

3. Discussion

The resource assessment with the presented method gives first (*a*) numerical results accompanied by a complementary purely (*b*) analytical approach similar to the approach of Vennell (2010*a*). However, instead of using the results of Garrett & Cummins (2007), the physically consistent model of Pelz *et al.* (2020) is used to close the gap of validity and to prevent overestimation of any energy yield. As shown by the combined experimental and theoretical research of Pelz *et al.* (2020) this is necessary for non-negligible water head differences, i.e. $\bar{h} < 0.95$, Froude numbers $Fr > 0.1$ or blockage ratios of at latest $\sigma > 0.5$.

The additional degree of freedom associated with the model of Pelz *et al.* (2020), i.e. the downstream boundary condition $\bar{h}$, is handled by proposing the relative volume flow q (1.1) as an operational parameter for the system instead of the often used induction factor a or turbine head $\bar{H}_T$. As q is implicitly dependent on the boundary condition $q = q(\bar{h})$, the influence of the latter on the relative power $p = p(q(\bar{h}))$ is negligible. In other words, p is only implicitly dependent on $\bar{h}$ as indicated by the above equation.

Furthermore, when considering turbine arrays, the volume flow q is identical for all fences, whereas induction factor α or turbine head $\bar{H}_T$ may differ (Schmitz & Pelz 2021). Instead of considering the momentum equation, the paper starts from the energy conservation. In this changed point of view, the system efficiency η is the leading characteristic to be tuned instead of the drag coefficient C_D. Due to $\eta \leqslant 1$, this naturally shows the limited power output of large turbine arrays, namely the power output of a zero-loss turbine fence, i.e. $\sigma = 1$, $\eta_T = 1 : \eta = 1$ as considered by Garrett & Cummins (2005).

By applying a simple rational approximation function, the paper gives a general and easy-to-use formula for the maximum power output of a more general turbine fence with partial blockage $0 \leqslant \sigma \leqslant 1$. This result may easily be adapted for regular arrays with multiple rows $L = 1, 2, 3, \ldots$. As a generalisation to Garrett & Cummins (2005), the presented work considers the influence of additional constraints like limited blockage, volume flow reduction or maximum realisable drag coefficient.

The paper aims to be a starting point for a physically consistent analysis of optimal flow control in tidal channels, as neither multiple fences nor a dynamical operation is considered. This is to be addressed in future work together with the dominating economical limits to the applicable number of turbines, i.e. the weighing up of the additional investment and operational costs vs the added revenue. For channels with dominant inductance and capacitance or for the latching control strategy proposed by Vennell (2016), the method needs further elaboration, taking the left-hand side of the Euler–Lagrange equation into account.

For channels with strong local effects, the generic model surely is insufficient. For those cases two-dimensional or three-dimensional fine-grained numerical models are needed as they are used already today. However, as these calculations are expensive, the presented model may serve as a first estimation in the early conceptual design phase of a project. It may also serve for a model predictive control strategy when operating a turbine array.

Funding. This research received no specific grant from any funding agency, commercial or not-for-profit sectors.

Declaration of interests. The authors report no conflict of interest.

Author ORCIDs.
Christian Schmitz https://orcid.org/0000-0002-7823-665X;
Peter F. Pelz https://orcid.org/0000-0002-0195-627X.

Appendix A. Three necessary conditions for quasi-steady channel flow

The system in question in this paper consists of two basins I and II, which are connected by a channel of length l and water depth h_0. The two basins are modelled as infinite in the context of this work. Therefore, the periodic volume flow in the channel $Q(t) = Q(t+T)$ has no feedback on the total energy heights $H_I(t) = H_I(t+T)$ and $H_{II}(t) = H_{II}(t+T)$ of the two basins. On the other hand, Q is of course a function of H_I and H_{II}. For the main part of this work, the answer to the question of whether the channel flow is unsteady or quasi-steady is crucial.

There are two approaches to answer this question. First, by a general dimensional analysis that provides the dimensionless products of the imposed frequency $f = 1/T \sim 10^{-4}$ Hz by the tides and the intrinsic time scales of the problem. Second, through an analysis of the magnitude of the dimensionless model equations. Pelz *et al.* (2022) have done this, by showing that the dimensionless products (2.5*a–c*) derived in the following serve as perturbation parameters of terms in the continuity and momentum equation that can be treated by methods known from regular or singular perturbation theory.

Provided the dimensionless products (2.5*a–c*) are small, the solution presented in the main part of this paper is in the context of perturbation theory a zero-order solution of the model equations. For the purpose of this paper, those solutions are sufficient in the first place. With no perturbation analysis in focus, it is sufficient to employ a general dimensional analysis.

For this, it is indeed helpful to use the electrical analogue of capacitance C, inductance L and resistance R of the flow, as it is already becoming known in the context of tidal power (Draper *et al.* 2014).

With C, L, R there are two intrinsic time scales $\sqrt{LC}$ and L/R and hence two dimensionless products $\Pi_1 := f\sqrt{LC}$, $\Pi_2 := f\,L/R$. One might think that there is a third dimensionless product $f\,RC$. This third product is given by $f\,RC = \Pi_1^2/\Pi_2$. Hence, its logarithm is linearly dependent on the logarithm of the other two products, known as

linear dependent dimensionless product in the context of dimensional analysis. When it comes to the order of magnitude analysis, all three products shall be smaller than one to justify the flow to be called quasi-stationary:

The first of the time scales, i.e. $\sqrt{LC}$, is the inverse of the eigenfrequency. The order of magnitude of this time scale is $\sqrt{LC} = l/\sqrt{(gh_0)} \sim (10^1 \ldots 10^3)$ s for typical tidal channels with water depth $h_0 \sim (10^1 \ldots 10^2)$ m and length $l \sim (10^3 \ldots 10^4)$ m. Hence, the first dimensionless product is, in fact, much smaller than one: $\Pi_1 := f\sqrt{LC} = fl/\sqrt{gh_0} \sim 10^{-3} \ldots 10^{-1}$. This magnitude analysis is already given by Pelz *et al.* (2020, 2022). It has been shown that $\Pi_1 \ll 1$ gives the magnitude of the unsteady terms in the dimensionless continuity and momentum equation as a perturbation parameter. Since the attention to Π_1 is not sufficient to judge whether a flow on a free surface is quasi-stationary or not, we extend the preceding analysis to completeness to obtain complete clarity regarding this question.

The second intrinsic time is the diffusion time $L/R = h_0^2/\nu$ needed for a velocity profile to develop across the channel depth, where ν is the kinematic viscosity. However, since the Reynolds number is high, $Re = h_0 u_0/\nu \sim 10^6$ for $u_0 \sim (1 \ldots 10)$ m s^{-1} and $\nu \approx 10^6$ m^2 s^{-1}, any viscous shear stress is negligible. Taking only turbulent shear stress τ_t into account, the diffusion time becomes h_0/u_* when the kinematic viscosity is replaced by the eddy viscosity $\nu_t \sim u_* h_0$. Here $u_* = \sqrt{\tau_t/\varrho}$ is the frictional velocity. Using von Kármán's log law $u_0/u_* \approx 0.4^{-1} \ln h_0/k + 5$ for an order of magnitude estimation of the frictional velocity $u_* \sim (0.2 \ldots 0.3)$ m s^{-1} for a seabed roughness of $k \sim (1 \ldots 10)$ cm, the order of magnitude of the diffusion time is $L/R = h_0^2/\nu_t \sim h_0/u_* \sim (10^1 \ldots 10^3)$ s. Hence, also the second dimensionless product is much smaller than one: $\Pi_2 := fL/R = fh_0/u_* \sim 10^{-3} \ldots 10^{-1}$; only for very deep channels, transient effects in the velocity distribution can become relevant.

The third and last intrinsic time scale is given by the relaxation time $RC = (l/h_0)^2 u_*/g \sim (10^1 \ldots 10^3)$ s. Hence, also the third and last (dependent) dimensionless product is much smaller than one: $\Pi_3 = \Pi_1^2/\Pi_2 = fRC = (l/h_0)^2 f u_*/g \sim 10^{-3} \ldots 10^{-1}$.

In summary, the time scales confirm that the flow in a typical tidal channel, which is the subject of this paper, is quasi-steady. Thus, time enters the problem only as a parameter in the boundary conditions $H_1(t) = H_I(t)$ and $h_2(t) = H_{II}(t)$.

Appendix B. Calculation flow diagram for the blockage-dependent power potential estimation

To assess the energy potential of a site, one only needs to know the amplitude of the head loss $\Delta\hat{H}$ and the undisturbed volume flow amplitude $\hat{Q}_0$ as well as, if existing, navigational, technical or ecological restrictions for the blockage ratio σ. Also there may be a constrained volume flow due to technical limitations as discussed above yielding q_{max}. The results may be further refined using the turbine efficiency η_T or a detailed conversion factor c to capture the specific time history of one tidal cycle $0 < t \leqslant T$.

The calculation flow diagram is given in figure 7. Using the head loss amplitude $\Delta\hat{H}$ and the undisturbed amplitude of the volume flow $\hat{Q}_0$, one may first calculate the maximal natural power dissipation within the channel $\hat{P}_{D,0}$, cf. step 1 in figure 7. It is easy to derive the maximum averaged extractable power, i.e. the power potential derived by Garrett & Cummins (2005) and the maximal meaningful volume flow reduction, cf. steps II, III in figure 7. In order to derive the power potential with restrictions applied, one first calculates the design constants D and d from the maximum possible blockage σ via (2.22) and

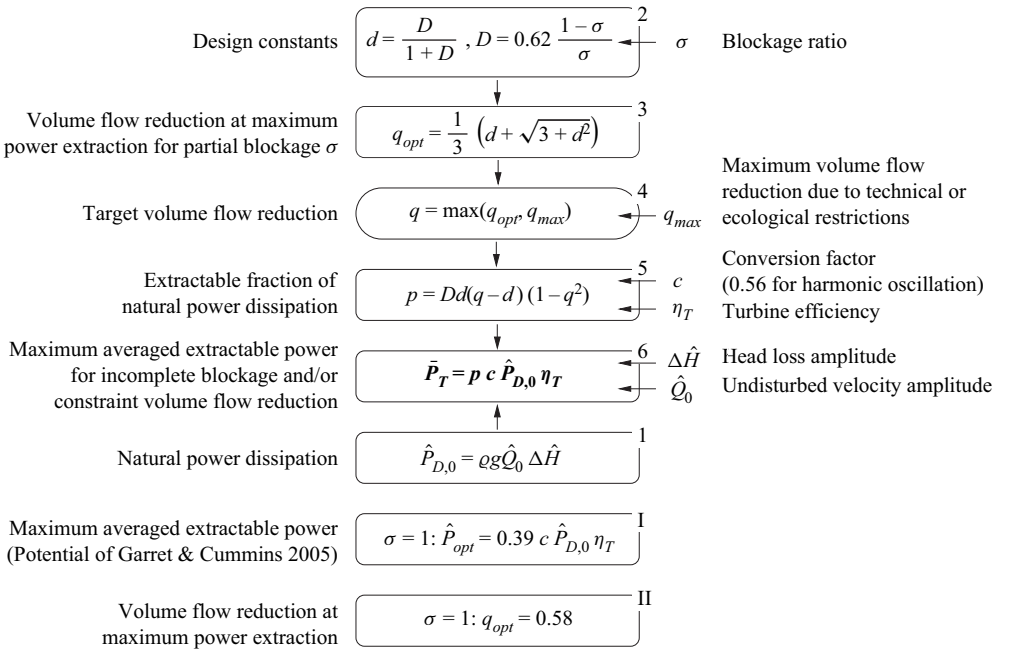

Figure 7. Calculation flow diagram for the blockage-dependent power potential estimation with process steps 1, 2, 3, 4, 5, 6, I and II.

(2.25), cf. step 2. This directly gives the optimal volume flow reduction for maximum power extraction q_{opt}, cf. (2.27), step 3, which may be limited by q_{max} due to further constraints, step 4. The resulting target volume flow reduction gives the extractable fraction of the natural power dissipation p via (2.10), step 5. Together with the reference $\hat{P}_{D,0}$ from step 1, the conversion factor $c \approx 0.56$, cf. § 2.6, and – if available – the turbine's efficiency η_T, this gives the maximum averaged extractable power for incomplete blockage and/or constraint volume flow reduction $\bar{P}_T$. Of course, the relative power p may as well be taken from figure 4 instead of steps 2 to 5.

References

Betz, A. 1920 Das Maximum der theoretisch möglichen Ausnutzung des Windes durch Windmotoren. *Zeitschrift für das gesamte Turbinenwesen* **26**, 307–309.

Black & Veatch Consulting Ltd 2005 Phase II UK tidal stream energy resource assessment. *Tech. Rep.* 107799/d/2200/03.

Bonar, P.A.J., Chen, L., Schnabl, A.M., Venugopal, V., Borthwick, A.G.L. & Adcock, T.A.A. 2019 On the arrangement of tidal turbines in rough and oscillatory channel flow. *J. Fluid. Mech.* **865**, 790–810.

Carbon Trust 2011 UK tidal current resource and economics.

Dehtyriov, D., Schnabl, A.M., Vogel, C.R., Draper, S., Adcock, T. & Willden, R.H. 2021 Fractal-like actuator disc theory for optimal energy extraction. *J. Fluid Mech.* **927**, A40.

Draper, S., Adcock, T.A.A., Borthwick, A.G.L. & Houlsby, G.T. 2014 An electrical analogy for the pentland firth tidal stream power resource. *Proc. R. Soc. Lond.* A **470**, 20130207.

ETSU 1993 Tidal stream energy review. *Tech. Rep*. ETSU-T-05/00155/REP, Harwell Laboratory, Energy Technology Support Unit, DTI.

Garrett, C. & Cummins, P. 2005 The power potential of tidal currents in channels. *Proc. R. Soc. Lond.* A **461** (2060), 2563–2572.

GARRETT, C. & CUMMINS, P. 2007 The efficiency of a turbine in a tidal channel. *J. Fluid Mech.* **588**, 243–251.

HOULSBY, G.T., DRAPER, S. & OLDFIELD, M.L.G. 2008 Application of linear momentum actuator disc theory to open channel flow. *Report No*. OUEL 2296 (08).

LANCHESTER, F.W. 1915 A contribution to the theory of propulsion and the screw propeller. *Trans. Inst. Nav. Archit.* **57**, 98–116.

NISHINO, T. & WILLDEN, R.H.J. 2012 The efficiency of an array of tidal turbines partially blocking a wide channel. *J. Fluid Mech.* **708**, 596–606.

NISHINO, T. & WILLDEN, R.H.J. 2013 Two-scale dynamics of flow past a partial cross-stream array of tidal turbines. *J. Fluid Mech.* **730**, 220–244.

OURO, P. & NISHINO, T. 2021 Performance and wake characteristics of tidal turbines in an infinitely large array. *J. Fluid Mech.* **925**.

PAHL, G., BEITZ, W., FELDHUSEN, J. & GROTE, K.-H. 2007 *Engineering Design*. Springer.

PELZ, P.F. 2011 Upper limit for hydropower in an open-channel flow. *ASCE J. Hydraul. Engng* **137** (11), 1536–1542.

PELZ, P.F., LEMMER, J. & SCHMITZ, C.B. 2022 Misled by Betz and unsteady flow – review on turbine arrays falsely deemed optimal. *Intl Mar. Energy J.* **5** (3), 239–247.

PELZ, P.F., METZLER, M., SCHMITZ, C.B. & MÜLLER, T.M. 2020 Upper limit for tidal power with lateral bypass. *J. Fluid. Mech.* **889**.

ROURKE, F.O., BOYLE, F. & REYNOLDS, A. 2010 Tidal energy update 2009. *Appl. Energy* **87**, 398–409.

SCHMITZ, C.B. & PELZ, P.F. 2021 Optimal operation of a regular turbine array in a generic tidal channel. In *The 14th European Wave and Tidal Energy Conference*.

VENNELL, R. 2010*a* Tuning turbines in a tidal channel. *J. Fluid Mech.* **663**, 253–267.

VENNELL, R. 2010*b* Tuning turbines in-concert to maximise farm efficiency. *J. Fluid Mech.* **671**, 587–604.

VENNELL, R. 2016 An optimal tuning strategy for tidal turbines. *Proc. R. Soc. Lond.* A **472**, 20160047.

VENNELL, R. & ADCOCK, T.A.A. 2013 Energy storage inherent in large tidal turbine farms. *Proc. R. Soc. Lond.* A **470**.

VOGEL, C.R., HOULSBY, G.T. & WILLDEN, R.H.J. 2016 Effect of free surface deformation on the extractable power of a finite width turbine array. *Renew. Energy* **88**, 317–324.

VOGEL, C.R., WILLDEN, R.H.J. & HOULSBY, G.T. 2019 Tidal stream turbine power capping in a head-driven tidal channel. *Renew. Energy* **136**, 491–499.

WHELAN, J.I., GRAHAM, J.M.R. & PEIRÓ, J. 2009 A free-surface and blockage correction for tidal turbines. *J. Fluid Mech.* **624**, 281–291.

WHELAN, J.I., THOMSON, M., GRAHAM, J.M.R. & PEIRÓ, J. 2007 Modelling of free surface proximity and wave induced velocities around a horizontal axis tidal stream turbine. In *Proceedings of the 7th European Wave and Tidal Energy Conference*.